

# Photochromism of Phenylazopyridines and Its Application to the Fluorescence Modulation of Zinc–Porphyrins

Joe Otsuki\* and Koichi Narutaki

College of Science and Technology, Nihon University, Kanda-Surugadai, Chiyoda-ku, Tokyo 101-8308

Received February 17, 2004; E-mail: otsuki@chem.cst.nihon-u.ac.jp

Several 2- and 3-(phenylazo)pyridine derivatives were prepared. Most of their *trans* isomers have a large absorption band ( $\sim 2 \times 10^4 \text{ M}^{-1} \text{ cm}^{-1}$  ( $1 \text{ M} = 1 \text{ mol dm}^{-3}$ )) around 320 nm and a small absorption band ( $\sim 400 \text{ M}^{-1} \text{ cm}^{-1}$ ) around 450 nm. All of these compounds photoisomerize upon irradiation of the shorter (*trans*-to-*cis*) and longer (*cis*-to-*trans*) wavelength absorption bands. *trans* Isomers of 3-(phenylazo)pyridines axially coordinate more strongly to Zn–porphyrins than *cis* isomers, while the opposite is the case for 2-(phenylazo)pyridines, due to steric reasons. These phenylazopyridines quench the fluorescence of Zn–porphyrin upon coordination. These properties were exploited for the light-triggered fluorescence modulation of Zn–porphyrins. Light was irradiated to a mixed solution of phenylazopyridine and Zn–porphyrin to induce photoisomerization of the phenylazopyridine, which underwent association with, or dissociation from, the Zn–porphyrin, resulting in a decrease or increase of Zn–porphyrin fluorescence. For example, the fluorescence intensity of Zn–tetraphenylporphyrin reversibly changed by up to 50%, when 4-methoxy-2-(phenylazo)pyridine was employed.

Manipulating electrons and photons at the molecular or supramolecular level are the aim of our research, motivated by the potential utility of molecule-based electronic and photonic devices.<sup>1</sup> Photoswitch, consisting of a luminescent center and a control unit that is responsive to an external trigger, is a device displaying interconversion between a non-luminescent state and a luminescent state effected by some external stimuli.<sup>2,3</sup>

We previously reported a non-covalent electron- and proton-responsive photoswitch wherein the fluorescence from a Zn–tetraphenylporphyrin (ZnTPP)–4-(phenylazo)pyridine (**4-Azo**) coordination complex is switched on/off responding to external redox or (de)protonation stimuli.<sup>4</sup> We later extended this approach to construct a non-covalent switch for energy transfer in a Zn–porphyrin–free-base porphyrin conjugate.<sup>5</sup> In these photoswitches, **4-Azo** was used as the control unit, since it quenches the fluorescence of ZnTPP nearly completely when axially bound, being able to make the “off” state. Once **4-Azo** is electrochemically reduced, its quenching ability is decreased and the fluorescence of ZnTPP is turned on. Alternatively, the addition of acid, which blocks the coordination site of **4-Azo**, i.e., pyridine-*N*, or base, which blocks the coordination site of ZnTPP, i.e., the central Zn ion, results in the dissociation of **4-Azo** from ZnTPP, giving rise to the fluorescence “on” state.

One of the problems associated with these photoswitches is that the signal homogeneity (e.g., light in, light out) is not maintained in their operation. The in-signal in these systems is a proton, electron, or a small molecule, while the out-signal is light. Signal homogeneity has to be maintained in order to arrange devices in tandem to make a logic array, in which the out-signal from the first device is used as the in-signal for the second device.<sup>6</sup>

The strategy that we employed here to overcome this problem is based on the photoisomerization and consequent steric

changes of phenylazopyridine derivatives, resulting in an alteration in binding affinity with Zn–porphyrins.<sup>7–9</sup> This strategy was previously used to control the chemical reactivity of porphyrins by switching the axial coordination state of stilbazole derivatives.<sup>10</sup> The *trans* isomer of 3-(phenylazo)pyridines would axially coordinate more strongly to Zn–porphyrins than the *cis* isomer, since one of the *cis* conformations cannot bind to Zn–porphyrins due to a steric hindrance, as illustrated in Fig. 1a. On the contrary, the *cis* isomer of 2-(phenylazo)pyridines would axially coordinate more strongly to Zn–porphyrins than the *trans* isomer, since only one of the *cis* conformations can bind without a steric hindrance to Zn–porphyrins, as illustrated in Fig. 1b. These phenylazopyridines quench the fluorescence of Zn–porphyrin upon coordination.<sup>4,5</sup> Thus, the light-induced isomerization of phenylazopyridine results in an increase/decrease of the coordination, leading to modulation of the porphyrin fluorescence. It has been confirmed that the proposed principle of operation is indeed workable, as demonstrated herein.<sup>11</sup>

## Results and Discussion

**Photochromism.** In this section, the photochromic properties of the phenylazopyridines used in the photoswitching study (Chart 1) are described. Aromatic azo compounds have been known for a long time, and still constitute active areas of investigation, in view of both their basic interest and their potential applications. The photochromism of azobenzene derivatives, among other properties, has attracted considerable attention.<sup>12–15</sup> The photochromic properties of azo chromophores containing heterocycles, such as pyridine,<sup>16,17</sup> however, have been much less explored than those of hydrocarbon counterparts.

UV–vis absorption features in toluene are tabulated in Table 1. The spectra for **Ph-3-Azo**, **MeO-2-Azo**, and **Me<sub>2</sub>N-3-Azo** are given in Fig. 2 as representative examples. The over-

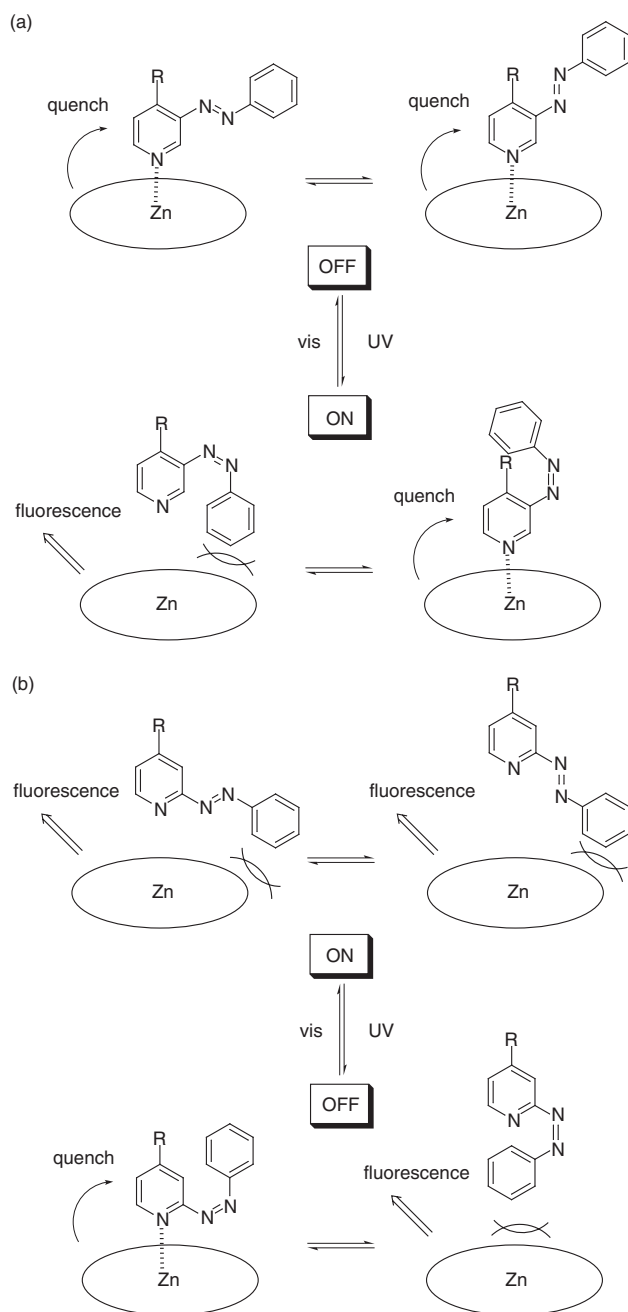


Fig. 1. The mode of operation for photoswitches or intensity modulation using (a) 3-(phenylazo)pyridines and (b) 2-(phenylazo)pyridines. Specific values of association constants are tabulated in Table 2.

all shape of the spectra for the other phenylazopyridines are more or less similar to those for the former two phenylazopyridines. The absorption spectra for these phenylazopyridines, except for **Me<sub>2</sub>N-3-Azo** (Fig. 2c), are characterized by strong, allowed  $\pi\pi^*$  transitions at 310–320 nm ( $\sim 2 \times 10^4 \text{ M}^{-1} \text{ cm}^{-1}$ ) and weak, forbidden  $n\pi^*$  transitions around 450 nm ( $\sim 400 \text{ M}^{-1} \text{ cm}^{-1}$ ).<sup>12,13</sup> It is noted that the  $\lambda_{\text{max}}$ 's of **Ph-3-Azo** are slightly red-shifted from those of others by about 10 nm, probably due to the extended  $\pi$  system.

In general, when irradiated at the shorter  $\lambda_{\text{max}}$  in the UV region, this higher energy absorption decreases, while the lower

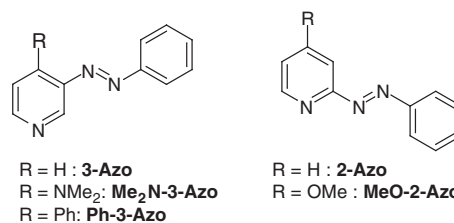


Chart 1.

energy absorption in the visible region increases, reaching a photostationary state, at which the *trans*/*cis* ratio becomes constant, depending on the irradiation wavelength. The photoisomerization reaction of **Ph-3-Azo** and **MeO-2-Azo** was probed by <sup>1</sup>H NMR spectroscopy (Fig. 3). A CDCl<sub>3</sub> solution of the *trans* isomer was irradiated to prepare a mixed solution of *trans* and *cis* isomers, for which <sup>1</sup>H NMR was taken. Generally, the resonances for the *cis* isomer appear at upper fields compared to those for the *trans* isomer. This may be explained mainly by the ring-current effect by the aromatic rings; the phenyl and pyridyl rings lie side-by-side in the *trans* isomer, while the two rings take, more or less, a face-to-face orientation in the *cis* isomer. Integration of the resonances gives the *trans*/*cis* ratio present in the solution. Therefore, the UV–vis spectra for pure *cis* isomers can be deduced by recording the UV–vis spectra for a mixed solution of known composition, which are included in Table 1 and Fig. 2. These data, in turn, allow one to estimate the *trans*/*cis* composition for any irradiated solutions. The thus-obtained *trans*/*cis* compositions under the photostationary states reached by irradiating at the shorter and longer  $\lambda_{\text{max}}$ 's are included in Table 1.

The spectrum for *trans*-**Me<sub>2</sub>N-3-Azo** is anomalous compared with others in that the short (313 nm) and long (404 nm) wavelength bands are of similar intensities. This is reflected in a unique behavior upon light irradiation. Both absorption bands decreased by irradiation at the longer  $\lambda_{\text{max}}$ , as shown in Fig. 2c. A subsequent irradiation at the shorter  $\lambda_{\text{max}}$  resulted in only a moderate increase in both absorption bands, indicating that the extent of reversible changes between the *trans* and *cis* forms is small under alternate irradiation.

**Axial Coordination of Phenylazopyridines and Fluorescence Quenching.** Phenylazopyridines form a 1:1 complex with Zn-porphyrins via axial coordination, not through the azo group, but through the nitrogen atoms in the pyridine ring, as was previously confirmed by <sup>1</sup>H NMR titration experiments.<sup>4,5</sup> A red-shift of the Soret and Q bands characterizes the complex formation.<sup>18</sup> Figure 4a shows the Q-band region of the UV–vis titration of Zn-tetramesitylporphyrin (ZnTMP) with *trans*-**Ph-3-Azo**. It is clear from the spectral change that the axially coordinated complex is formed, although isosbestic points are blurred by the absorption tail of *trans*-**Ph-3-Azo**. From the change in the absorption spectra upon the addition of *trans*-phenylazopyridines, the association constants were evaluated by using a least-squares curve-fitting procedure. The results are summarized in Table 2. The *trans* isomer of **3-Azo** forms a complex with ZnTPP with an association constant of  $1590 \text{ M}^{-1}$  in toluene at 25 °C. Substitution at the 4-position of the pyridine ring in **3-Azo** by phenyl and dimethylamino groups results in 5- and 33-fold increases, respectively,

Table 1. Properties of Phenylazopyridines<sup>a)</sup>

	$\lambda_{\max}/\text{nm}$ ( $\epsilon/\text{M}^{-1}\text{cm}^{-1}$ )	pss(s) <sup>b)</sup>	pss(l) <sup>c)</sup>	$E_{1/2}/\text{V}^{\text{d)}$
<i>trans</i> -3-Azo	320 (21000), 449 (480)	n.d.	n.d.	−1.63
<i>trans</i> -Me <sub>2</sub> N-3-Azo	313 (7400), 404 (5200)	n.d.	n.d.	−1.84
<i>trans</i> -Ph-3-Azo	326 (18000), 465 (310)	0.31	0.90	−1.62
<i>cis</i> -Ph-3-Azo	<300, 440 (950)	0.69	0.10	n.d.
<i>trans</i> -2-Azo	318 (18000), 454 (390)	n.d.	n.d.	−1.58
<i>trans</i> -MeO-2-Azo	315 (16000), 451 (350)	0.19	0.93	−1.68
<i>cis</i> -MeO-2-Azo	<300, 436 (860)	0.81	0.07	n.d.

a) In toluene at 25 °C. b) Ratios of *trans*/*cis* forms at the photostationary state under the shorter wavelength irradiation. c) Ratios of *trans*/*cis* forms at the photostationary state under the longer wavelength irradiation. d) Reduction potentials (vs Fc<sup>+</sup>/Fc) in CH<sub>2</sub>Cl<sub>2</sub> containing 0.1 M Bu<sub>4</sub>NPF<sub>6</sub>.

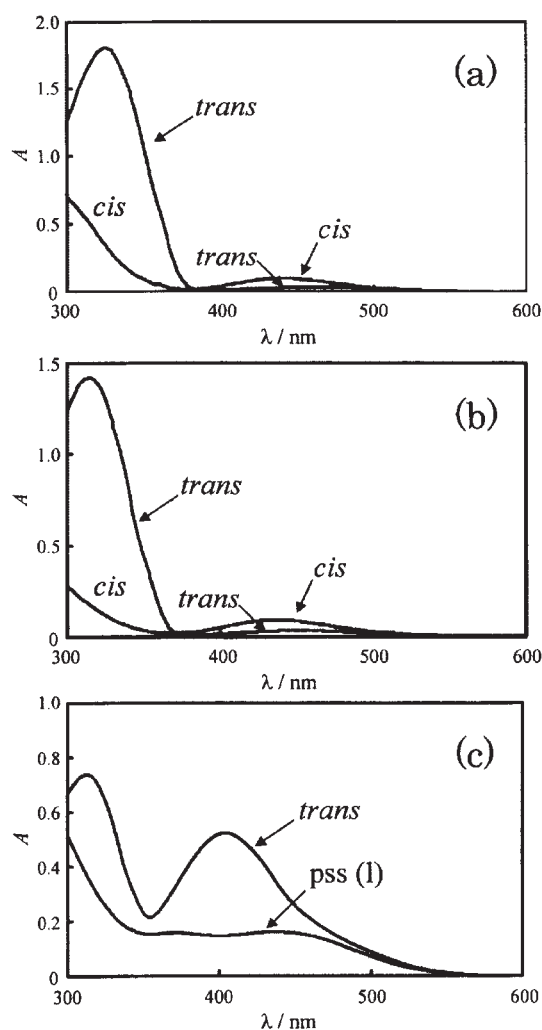


Fig. 2. UV-vis absorption spectra for phenylazopyridines (0.1 mM) in toluene at 25 °C: (a) *trans*- and *cis*-Ph-3-Azo, (b) *trans*- and *cis*-MeO-2-Azo, and (c) *trans*-Me<sub>2</sub>N-3-Azo and its photostationary state under 404-nm irradiation (pss(l)).

in the binding affinity toward ZnTPP.

The coordination of *trans*-2-Azo to ZnTPP is almost negligible. The introduction of a methoxy group to the 4-position of the pyridine ring does increase the affinity. However, the association constant between *trans*-MeO-2-Azo and ZnTPP is still very low ( $\sim 10\text{ M}^{-1}$ ). One of the reasons for the large difference

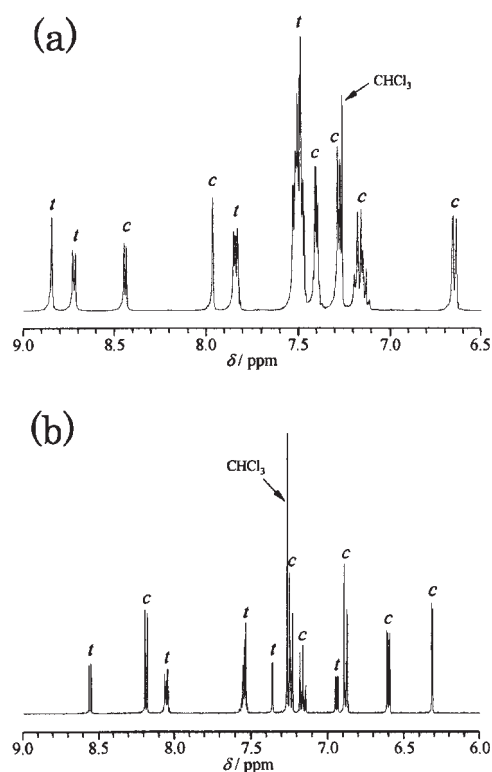


Fig. 3. <sup>1</sup>H NMR spectra for a mixture of *trans*- (*t*) and *cis*- (*c*) phenylazopyridines in CDCl<sub>3</sub>: (a) Ph-3-Azo; (b) MeO-2-Azo (the resonances for methoxy protons are omitted).

in the binding affinity between 3- and 2-(phenylazo)pyridines is apparently steric; the phenylazo group at the 2-position of the pyridine ring hinders the coordinating pyridine-*N* more effectively (see Fig. 1).

The formation of axially coordinated complexes is accompanied by the quenching of porphyrin fluorescence. The relative fluorescence intensity of ZnTPP is plotted against the concentration of added *trans*-Ph-3-Azo, as shown in Fig. 4b. Also included in the same graph is the ratio of free ZnTPP as a function of the added *trans*-Ph-3-Azo concentration, based on the association constant obtained by the absorption changes as described above. A comparison of these two curves allows a quantitative estimation of the relative fluorescence intensity of the complex, *trans*-Ph-3-Azo·ZnTPP, as 0.07. Thus, 93% of the fluorescence of ZnTPP is quenched in the complex by

Table 2. Interactions of Phenylazopyridines with Zn-Porphyrins<sup>a)</sup>

Compound	Porphyrin	$K_{\text{trans}}/\text{M}^{-1}$	$K_{\text{cis}}/\text{M}^{-1}$	$\phi_{\text{q}}^{\text{b)}}$	On/off ratio	$\Delta G/\text{eV}^{\text{c)}}$
<b>3-Azo</b>	ZnTPP	1590 <sup>d)</sup>	n.d.	0.94	1/0.9	-0.18
<b>Me<sub>2</sub>N-3-Azo</b>	ZnTPP	52000 <sup>d)</sup>	n.d.	0.58	1/0.95	0.03
<b>Me<sub>2</sub>N-3-Azo</b>	ZnTMP	101000 <sup>d)</sup>	n.d.	0.53	1/0.86	0.40
<b>Ph-3-Azo</b>	ZnTPP	7390 <sup>d)</sup>	5000 ( $\pm$ 400)	0.89	1/0.86	-0.19
<b>Ph-3-Azo</b>	ZnTMP	15900 <sup>d)</sup>	1600 ( $\pm$ 400)	0.93	1/0.8	0.18
<b>2-Azo</b>	ZnTPP	<10	n.d.	n.d.	1/1	-0.23
<b>MeO-2-Azo</b>	ZnTPP	$\sim$ 10	90 ( $\pm$ 20)	n.d.	1/0.55	-0.13

a) In toluene at 25 °C. b) Efficiencies of quenching of Zn-porphyrin fluorescence when bound. c) Free energy changes upon electron transfer from the singlet excited state of Zn-porphyrin to phenylazopyridine. d) Conditional standard deviations are  $<\pm 1\%$ .

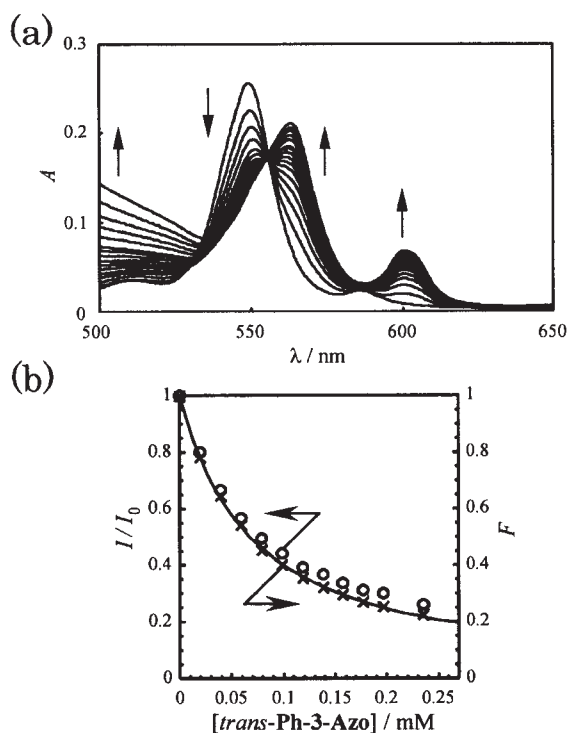


Fig. 4. Spectral changes for a solution of ZnTMP (10  $\mu\text{M}$ ) in toluene upon addition of *trans*-Ph-3-Azo at 25 °C. (a) Changes in the Q-band region of the UV-vis spectrum for ZnTMP. (b) Fractions ( $F$ ) of free ZnTMP to the total ZnTMP concentrations (line and crosses) are compared with relative fluorescence intensities (circles) as a function of added *trans*-Ph-3-Azo in the same experiment as in (a).  $\lambda_{\text{ex}} = 585 \text{ nm}$  (isosbestic point).

the presence of *trans*-Ph-3-Azo. The quenching efficiencies,  $\phi_{\text{q}}$ , thus obtained for other combinations of 3-(phenylazo)pyridines and porphyrins are displayed in Table 2.

In general, the quenching of an excited state is due to additional relaxation pathways such as electron transfer or energy transfer. Energy-transfer quenching in the present case is unlikely, since the excited-state energies of azopyridines, e.g., 2.63 eV for *trans*-3-Azo, as estimated with ZINDO calculations, are much larger than those of porphyrins (2.04–2.05 eV). Although it is suggested that non-vertical energy transfer is involved in triplet manifolds in axially-bound porphyrin–stilbazole systems,<sup>19</sup> it is not clear whether such a non-vertical

process is feasible for singlet energy transfer.

The free-energy changes ( $\Delta G$ ) upon electron transfer from the singlet excited-state of Zn-porphyrins to phenylazopyridines were calculated using Eq. 1, and are summarized in Table 2.

$$\Delta G = E_{\text{D}^+/\text{D}} - E_{00} - E_{\text{A}/\text{A}^-}. \quad (1)$$

Values used in the calculation of  $\Delta G$  are the reduction potentials ( $E_{\text{A}/\text{A}^-}$ ) of azo compounds, which are tabulated in Table 1, the oxidation potentials ( $E_{\text{D}^+/\text{D}}$ ) of axially-coordinated ZnTPP (0.30 V vs  $\text{Fc}^+/\text{Fc}$ ) and ZnTMP (0.61 V), and the singlet excited-state energies ( $E_{00}$ ) of axially-coordinated ZnTPP (2.04 eV) and ZnTMP (2.05 eV). In the calculation, it was taken into account that the redox potentials of azo compounds change upon axial coordination to ZnTPP (but not for ZnTMP) by +70 mV. The obtained  $\Delta G$ 's have to be considered as relative values, however, since the electrostatic stabilization term for the charge separated state, which could amount to several tenths eV, was not included due to uncertainties in parameters, such as the donor–acceptor separation. It is clear, though, that the quenching efficiency is significantly lower for *trans*-Me<sub>2</sub>N-3-Azo, which has a more negative reduction potential, than *trans*-3-Azo and *trans*-Ph-3-Azo, being consistent with the electron-transfer mechanism. Electron-transfer quenching is also consistent with the previously reported fact that the electrochemical reduction of 4-Azo deprives its quenching ability.<sup>4</sup>

However, the fluorescence of ZnTMP, which has a more positive oxidation potential than ZnTPP by as much as 0.3 V, is quenched to an extent comparable to that of ZnTPP by the same phenylazopyridines, which is unlikely if electron transfer is the sole mechanism of quenching, since factors affecting the electron-transfer rate, such as donor–acceptor separation, orientation, and reorganization energy, are considered to be similar in these porphyrin–azopyridine systems. One possibility is that changes in the conformational distributions of the mesityl and phenyl rings upon binding to azopyridine are different for these porphyrins, non-radiative decay pathways being potentially modulated to different extents. Further study is needed to clarify the mechanism of the quenching of Zn-porphyrin fluorescence by phenylazopyridines.

#### Fluorescence Modulation Using 3-(Phenylazo)pyridines.

As explained in the introduction, it is expected that 3-(phenylazo)pyridines axially coordinate to Zn-porphyrin more strongly, and hence quench its fluorescence in the *trans* form than in the *cis* form more effectively. Thus, light-induced isomeriza-



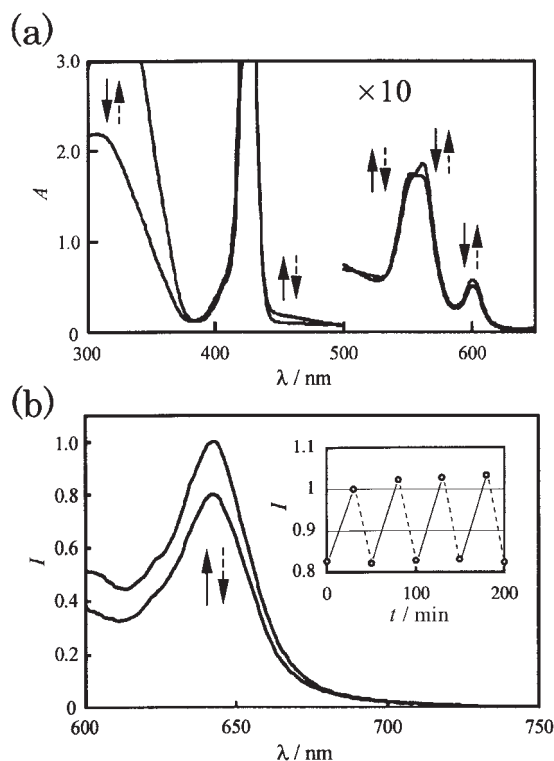


Fig. 5. Irradiation-induced spectral changes for a solution of **Ph-3-Azo** (0.25 mM) and ZnTMP (10  $\mu$ M) in toluene at 25  $^{\circ}$ C. Solid arrows represent changes associated with *trans*-to-*cis* isomerization upon 326-nm irradiation, while dotted arrows represent the opposite process upon 442-nm irradiation. (a) Absorption spectra. (b) Fluorescence spectra ( $\lambda_{\text{ex}} = 585$  nm). The inset shows fluorescence intensity variations on the repetition of alternate irradiation. Solid and dotted lines represent 326- and 442-nm irradiation, respectively.

tion of 3-(phenylazo)pyridines would result in the increase/decrease of the porphyrin fluorescence.

The experiment of porphyrin fluorescence modulation will be illustrated using the case involving **Ph-3-Azo** and ZnTMP as a representative example. A solution of *trans*-**Ph-3-Azo** (0.25 mM) and ZnTMP (10  $\mu$ M) in toluene was prepared, in which the amount of the complex, *trans*-**Ph-3-Azo**·ZnTMP, was estimated from the association constant (15900  $\text{M}^{-1}$ ) to be 7.9  $\mu$ M or 79% of the total porphyrin molecules. This solution was irradiated by 326-nm light until the spectrum became constant (20–30 min). A large decrease in the absorbance around 300–380 nm and a slight increase around 450–500 nm in the UV–visible spectrum upon irradiation showed that *trans*-**Ph-3-Azo** photoisomerized into the *cis* form, see Fig. 5a. The ratio of the *trans* and *cis* forms in this photostationary state under these conditions was *trans*/*cis* = 33/67. Concomitant with these spectral changes due to the azo compound, the Q-band of ZnTMP also exhibited changes in the direction indicative of a dissociation of the axial ligand. The amount of complex, **Ph-3-Azo**·ZnTMP, at this photostationary state was estimated from the shape of the spectrum to be  $\sim 6.5$   $\mu$ M. During the irradiation, until the photostationary state was reached, the time course of the absorption spectra was recorded, which gives

the amounts of axially-coordinated ZnTMP, *trans*-, and *cis*-**Ph-3-Azo**. The association constant of *cis*-**Ph-3-Azo** and ZnTMP ( $K_{\text{cis}}$ ) was estimated to be 1600 ( $\pm 400$ )  $\text{M}^{-1}$  using these data points and the known value of  $K_{\text{trans}}$ . Thus, it has been demonstrated that the association constant decreases by an order of magnitude when *trans*-**Ph-3-Azo** changes into its *cis* form. Subsequent irradiation at 442 nm reversed all of the changes described above, indicating the *cis*-to-*trans* conversion of **Ph-3-Azo** and a simultaneous increase of the bound species, **Ph-3-Azo**·ZnTMP.

The fluorescence from ZnTMP was monitored by excitation at 585 nm, one of the isosbestic points, during the cycle of irradiation; the results are shown in Fig. 5b. The fluorescence was enhanced upon 326-nm irradiation and diminished upon 442-nm irradiation. The former process corresponds to the *trans*-to-*cis* conversion and related dissociation of **Ph-3-Azo** from ZnTMP, while the latter corresponds exactly to the opposite process. These changes were reasonably reversible, as shown in the inset of Fig. 5b. The on/off ratio, defined as the ratio of the fluorescence intensities at the photostationary states under the longer and shorter wavelength irradiation, was 1/0.8. Thus, a new mode of operation is demonstrated for light-responsive fluorescence modulation based on non-covalent assemblies.

The on/off ratios for the other 3-(phenylazo)pyridines are summarized in Table 2. Briefly, the on/off ratio for **Me<sub>2</sub>N-3-Azo** is small, since the extent of change between the *trans* and *cis* forms is small (vide supra). The on/off ratio for **Ph-3-Azo** is the largest, since the presence of a phenyl group at the 4-position of the pyridine ring disfavors the conformation shown in the lower right in Fig. 1a. Hence, the dissociation of the *cis* form is more facilitated than for the case of **3-Azo**. This is particularly the case when ZnTMP is used as the porphyrin unit, since *ortho*-methyl groups on the *meso*-phenyl groups provide an enhanced steric hindrance to *cis*-**Ph-3-Azo**.

#### Fluorescence Modulation Using 2-(Phenylazo)pyridines.

2-(Phenylazo)pyridines are expected to axially coordinate to Zn–porphyrin more strongly, and hence quench its fluorescence in the *cis* form than in the *trans* form due to steric reasons. Thus, the system involving 2-(phenylazo)pyridines is complementary to that involving 3-(phenylazo)pyridines.

The absorption spectrum for *trans*-**2-Azo** exhibits peaks at 318 and 454 nm (Table 1). Upon excitation at 318 nm, it isomerized into the *cis* form. However, neither *trans*- nor *cis*-**2-Azo** axially coordinated to ZnTPP in toluene to a detectable extent, even when a large excess of **2-Azo** (e.g., 15 mM) was used. This is not due to steric reasons, since *cis*-2-stilbazole does coordinate to Zn–porphyrins.<sup>10a</sup> The lack of a coordination ability of *cis*-**2-Azo** may be attributed to its smaller  $\text{p}K_{\text{a}}$  value (2.0)<sup>20</sup> compared to that of 2-stilbazole (5.0).<sup>21</sup> Thus, substitution by an electron-donating group was necessary to confer the azo compound a coordinating ability, which guided us to the preparation of **MeO-2-Azo**.

An inspection of the absorption spectrum of a toluene solution containing *trans*-**MeO-2-Azo** (20 mM) and ZnTPP (1 mM) showed that only a small fraction of ZnTPP was axially coordinated, even with relatively high *trans*-**MeO-2-Azo** concentrations. Indeed, the UV–vis titration of ZnTPP with *trans*-**MeO-2-Azo** showed that the association constant is of the order

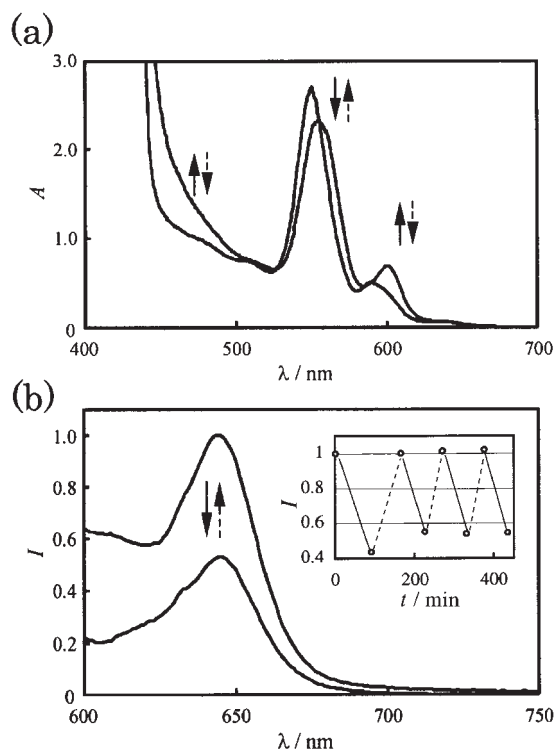


Fig. 6. Irradiation-induced spectral changes for a solution of **MeO-2-Azo** (20 mM) and ZnTPP (1 mM) in toluene at 25 °C. Solid arrows represent changes associated with *trans*-to-*cis* isomerization upon 315-nm irradiation, while dotted arrows represent the opposite process upon 436-nm irradiation. (a) Absorption spectra (1 mm  $\times$  1 cm cell). (b) Fluorescence spectra ( $\lambda_{\text{ex}}$  = 585 nm). The inset shows fluorescence intensity variations on the repetition of alternate irradiation. Solid and dotted lines represent 315- and 436-nm irradiation, respectively.

of 10 M<sup>-1</sup>. Upon irradiation at 318 nm, the absorption around 450 nm increased, indicating that *trans*-to-*cis* isomerization took place (see Fig. 6a). Concomitant with this spectral change, the Q band of ZnTPP was red-shifted, indicating that axial coordination took place at the same time. Thus, *cis*-**MeO-2-Azo** coordinates to ZnTPP more strongly than its *trans* counterpart. About 50% of ZnTPP was estimated to be coordinated from the shape of the Q band at the photostationary state under 318-nm irradiation. The association constant between *cis*-**MeO-2-Azo** and ZnTPP was estimated to be 90 ( $\pm$  20) M<sup>-1</sup> in a similar fashion as demonstrated for **Ph-3-Azo**. It is thus demonstrated again that about an order of magnitude difference in binding affinity of the *trans* and *cis* forms to Zn-porphyrin. The spectral changes are reversible; a 436-nm irradiation to the solution containing the *cis* form resulted in the recovery of the original spectrum, indicating both *cis*-to-*trans* isomerization and detachment of **MeO-2-Azo** from ZnTPP took place.

The fluorescence from ZnTPP was monitored by excitation at 585 nm, one of the isosbestic points, during the cycle of irradiation. The fluorescence decreased upon binding of **MeO-2-Azo** down to ca. 50% of the initial intensity at the photostationary state (Fig. 6b); an on/off ratio of 1/0.5 was achieved. At this photostationary state, ~50% of ZnTPP is axially coordinated, while the fluorescence intensity is ~50% of that of ZnTPP

alone. This means that the quenching efficiency of **MeO-2-Azo** is as high as being close to unity, although an exact estimation is difficult. The fluorescence change is reversible as well; the original intensity was recovered upon re-irradiation at 436 nm. Several cycles of alternate irradiation and the fluorescence response is illustrated in the inset of Fig. 6b. It is thus concluded that the system employing 2-(phenylazo)pyridines can also be used to modulate the intensity of porphyrin fluorescence. The behavior of attachment and detachment of 2-(phenylazo)pyridines with Zn-porphyrins in response to light irradiation is exactly the opposite to, thus complementary to, that of 3-(phenylazo)pyridines.

## Conclusion

In this article, we have described the basic properties of several photochromic phenylazopyridine derivatives. We have also demonstrated an application of these photochromic compounds to the modulation of porphyrin fluorescence.

*cis* Isomers of 2-(phenylazo)pyridines axially coordinate more strongly to Zn-porphyrins than *trans* isomers, and hence quench more effectively porphyrin fluorescence, while the opposite is the case for 3-(phenylazo)pyridines. Thus, a complementary set of photomodulation systems that responds to a light trigger is demonstrated. In particular, an on/off ratio of 1/0.5 was achieved using the combination of **MeO-2-Azo** and ZnTPP.

This is an important step toward molecular devices that process photon-based information, since the signal homogeneity is now maintained. An output light from a device may be, in principle, used as an input signal for the next device, opening a way toward the integration of devices. However, a number of issues have to be addressed before the practical implementation of this system, further improvement of the on/off ratio being among the most important.

Finally, it may be worth noting that all of the phenylazopyridines studied here showed photoisomerization in the presence of porphyrins. One of the advantages to use the non-covalent strategy is that photoisomerization is assured in these systems, since there are always free azo molecules that are not bound to porphyrin, and hence, whose photophysics is not affected by the presence of porphyrin. In covalent porphyrin-azobenzene systems, or systems in which a photochromic unit is covalently linked with another electro- or photo-active group in general, it has sometimes been observed that the photochromic component is so perturbed that it no longer undergoes photoisomerization.<sup>6,22</sup>

## Experimental

**Instruments.** <sup>1</sup>H NMR spectra were recorded on a JEOL JNM-GX400 spectrometer. EIMS spectra were taken with a Shimadzu GCMS-QP5050 spectrometer equipped with a direct injection unit. FABMS spectra measurements were done by I. Yoshikawa of the University of Tokyo. Elemental analyses were performed by the Chemical Analysis Center of the College of Science and Technology, Nihon University.

UV-vis and fluorescence data were obtained using Shimadzu UV-2400PC and RF-5300PC spectrophotometers, respectively. Photoisomerization experiments were carried out in a 1 cm  $\times$  1 cm or 1 mm  $\times$  1 cm quartz cell maintained at 25 °C by irradiation.

tion with the light source of a spectrometer (RF-5300PC) with a slit width of 20 nm. Fluorescence spectra was measured with a vertical mode and a surface reflectance mode for the 1 cm × 1 cm and 1 mm × 1 mm cells, respectively. The 1-mm optical cell was used only in the photomodulation experiment with **MeO-2-Azo** shown in Fig. 6. Cyclic voltammetry was carried out with a Hokuto Denko HZ-3000 voltammetric analyzer. The electrochemical cell, maintained under N<sub>2</sub>, was equipped with a Pt disk working electrode, a Pt-wire counter electrode, and an Ag/Ag<sup>+</sup> reference electrode. The supporting electrolyte solution was 0.1 M Bu<sub>4</sub>NPF<sub>6</sub> in CH<sub>2</sub>Cl<sub>2</sub>. Potentials are reported with respect to the internal Fc<sup>+</sup>/Fc couple, added after each measurement.

The singlet excited-state energies for azopyridines were calculated for geometry-optimized structures by the ZINDO method using INDO/1 parameters with configuration interaction level 14 in the CAChe package.<sup>23</sup>

**Materials.** Spectroscopic grade toluene was purchased from Wako Pure Chemical. **2-Azo** and **3-Azo** were prepared from 2- and 3-aminopyridine, respectively, and nitrosobenzene.<sup>16</sup> **MeO-2-Azo**<sup>24</sup> was prepared similarly from 2-amino-4-methoxypyridine<sup>25</sup> and nitrosobenzene.

**Me<sub>2</sub>N-3-Azo.** Nitrosobenzene (170 mg, 1.59 mmol) was added portionwise to a well-stirred two-phase mixture of aqueous NaOH (5.8 g/5 mL) and a solution of 3-amino-4-dimethylaminopyridine<sup>26</sup> (195 mg, 42 mmol) in benzene (1 mL) at 90 °C. After 25 min, the reaction mixture was extracted with benzene, which was dried over MgSO<sub>4</sub> and evaporated. The residue was purified on a preparative alumina TLC plate using CH<sub>2</sub>Cl<sub>2</sub> as an eluent. The material collected from the central orange band was freeze-dried from benzene to afford **Me<sub>2</sub>N-3-Azo** as orange powder (20 mg, 6%). <sup>1</sup>H NMR (CDCl<sub>3</sub>) δ 8.52 (1H, s), 8.22 (1H, d, *J* = 6 Hz), 7.85 (2H, d, *J* = 7 Hz), 7.43–7.53 (3H, m), 6.71 (1H, d, *J* = 6 Hz), 3.26 (6H, s). EIMS: *m/z* = 226 (M<sup>+</sup>). Anal. Found: C, 68.85; H, 6.28; N, 24.60%. Calcd for C<sub>13</sub>H<sub>14</sub>N<sub>4</sub>: C, 69.00; H, 6.24; N, 24.76%.

**3-Amino-4-phenylpyridine.** This compound was previously obtained by the reduction of 3-nitro-4-phenylpyridine,<sup>27</sup> which was prepared by nitration of 4-phenylpyridine by the reaction with N<sub>2</sub>O<sub>5</sub> followed by an aqueous solution of SO<sub>2</sub> or NaHSO<sub>3</sub>.<sup>11,28</sup> 3-Nitro-4-phenylpyridine was also prepared by a standard Suzuki coupling procedure<sup>29</sup> from 4-chloro-3-nitropyridine<sup>30</sup> and phenylboronic acid. Reduction of this nitro compound with Fe powder in acetic acid<sup>26b</sup> afforded 3-amino-4-phenylpyridine.

**Ph-3-Azo.** Nitrosobenzene (183 mg, 1.71 mmol) was added portionwise to a well-stirred two-phase mixture of aqueous NaOH (5 g/5 mL) and a solution of 3-amino-4-phenylpyridine (202 mg, 1.18 mmol) in benzene (2 mL) at 90 °C. After 25 min, the reaction mixture was extracted with benzene, which was dried over MgSO<sub>4</sub> and evaporated. The residue was purified on a preparative alumina TLC plate using CH<sub>2</sub>Cl<sub>2</sub>/hexane (1:1) as an eluent. The central orange band was collected to afford **Ph-3-Azo** as orange powder (83 mg, 27%). <sup>1</sup>H NMR (CDCl<sub>3</sub>) δ 8.85 (1H, s), 8.72 (1H, d, *J* = 5.2 Hz), 7.96–7.82 (2H, m), 7.53–7.46 (9H, m). FABMS: *m/z* = 260 (MH<sup>+</sup>). Anal. Found: C, 78.69; H, 5.29; N, 16.12%. Calcd for C<sub>17</sub>H<sub>13</sub>N<sub>3</sub>: C, 78.74; H, 5.05; N, 16.20%.

This work was funded by the High-Tech Research Center of Nihon University, Institute of Quantum Science of Nihon University, and Saneyoshi Scholarship Foundation. We thank I. Yoshikawa of the University of Tokyo for FABMS measurements.

## References

- 1 C. Joachim, J. K. Gimzewski, and A. Aviram, *Nature*, **408**, 541 (2000).
- 2 a) J.-M. Lehn, "Supramolecular Chemistry," VCH, Weinheim (1995). b) J.-M. Lehn, *Angew. Chem., Int. Ed. Engl.*, **29**, 1304 (1990).
- 3 V. Goulle, A. Harriman, and J.-M. Lehn, *J. Chem. Soc., Chem. Commun.*, **1993**, 1034.
- 4 J. Otsuki, K. Harada, and K. Araki, *Chem. Lett.*, **1999**, 269.
- 5 J. Otsuki, A. Yasuda, and T. Takido, *Chem. Commun.*, **2003**, 608.
- 6 A. J. Myles and N. R. Branda, *J. Am. Chem. Soc.*, **123**, 177 (2001).
- 7 G. Cooke, *Angew. Chem., Int. Ed.*, **42**, 4860 (2003).
- 8 M. Lahav, K. T. Ranjit, E. Katz, and I. Willner, *Chem. Commun.*, **1997**, 259.
- 9 M. J. Cook, A.-M. Nygård, Z. Wang, and D. A. Russell, *Chem. Commun.*, **2002**, 1056.
- 10 a) Y. Iseki, E. Watanabe, A. Mori, and S. Inoue, *J. Am. Chem. Soc.*, **115**, 7313 (1993). b) Y. Iseki and S. Inoue, *J. Chem. Soc., Chem. Commun.*, **1994**, 2577. c) H. Sugimoto and S. Inoue, *Pure Appl. Chem.*, **70**, 2365 (1998). d) H. Sugimoto, T. Kimura, and S. Inoue, *J. Am. Chem. Soc.*, **121**, 2325 (1999).
- 11 Part of this work was published in a preliminary communication: J. Otsuki, K. Narutaki, and J. M. Bakke, *Chem. Lett.*, **33**, 356 (2004).
- 12 H. Rau, "Studies in Organic Chemistry 40: Photochromism: Molecules and Systems," ed by H. Dürr and H. Bouas-Laurent, Elsevier, Amsterdam (1990), Chap. 4, p. 165.
- 13 B. L. Feringa, W. F. Jager, and B. de Lange, *Tetrahedron*, **49**, 8267 (1993).
- 14 I. Willner and S. Rubin, *Angew. Chem., Int. Ed. Engl.*, **35**, 367 (1996).
- 15 S. Makita, A. Saito, M. Hayashi, S. Yamada, K. Yoda, J. Otsuki, T. Takido, and M. Seno, *Bull. Chem. Soc. Jpn.*, **73**, 1525 (2000).
- 16 E. V. Brown and G. R. Granneman, *J. Am. Chem. Soc.*, **97**, 621 (1975).
- 17 W. A. Sokalski, R. W. Góra, W. Bartkowiak, P. Kobylinski, J. Sworakowski, A. Chyla, and J. Leszczyński, *J. Chem. Phys.*, **114**, 5504 (2001).
- 18 J. Otsuki, *Trends Phys. Chem.*, **8**, 61 (2001).
- 19 a) D. G. Whitten, I. G. Lopp, and P. D. Wildes, *J. Am. Chem. Soc.*, **90**, 7196 (1968). b) D. G. Whitten, P. D. Wildes, and I. G. Lopp, *J. Am. Chem. Soc.*, **91**, 3393 (1969). c) P. D. Wildes and D. G. Whitten, *J. Am. Chem. Soc.*, **92**, 7609 (1970). d) D. G. Whitten, P. D. Wildes, and C. A. DeRosier, *J. Am. Chem. Soc.*, **94**, 7811 (1972).
- 20 A. Foffani and M. R. Foffani, *Atti Accad. Naz. Lincei, Cl. Sci. Fis., Mat. Nat., Rend.*, **23**, 60 (1957).
- 21 G. Cauzzo, G. Gializzo, U. Mazzucato, and N. Mongiat, *Tetrahedron*, **22**, 589 (1966).
- 22 C. A. Hunter and L. D. Sarson, *Tetrahedron Lett.*, **37**, 699 (1996).
- 23 M. C. Zerner, ZINDO program, Quantum Theory Project, University of Florida, Gainesville, FL, USA, 1998.
- 24 M. N. Ackermann, W. G. Fairbrother, N. S. Amin, C. J. Deodene, C. M. Lamborg, and P. T. Martin, *J. Organomet. Chem.*, **523**, 145 (1996).
- 25 R. J. Sundberg and S. Jiang, *Org. Prep. Proced. Int.*, **29**, 117 (1997).

26 a) A. G. Burton, R. D. Frampton, C. D. Johnson, and A. R. Katritzky, *J. Chem. Soc., Perkin Trans. 2*, **1972**, 1940. b) D. Rasala, *Bull. Soc. Chim. Fr.*, **129**, 79 (1992).

27 J. M. Bakke and J. Riha, *J. Heterocycl. Chem.*, **38**, 99 (2001).

28 J. M. Bakke, E. Ranes, J. Riha, and H. Svensen, *Acta Chem.*

*Scand.*, **53**, 141 (1999).

29 R. Crous, C. Dwyer, and C. W. Holzapel, *Heterocycles*, **51**, 721 (1999).

30 M. F. Reich, P. F. Fabio, V. J. Lee, N. A. Kuck, and R. T. Testa, *J. Med. Chem.*, **32**, 2474 (1989).